

Presence of Dark Energy and Dark Matter : Does Cosmic Acceleration signifies a Weak Gravitational collapse?

Prabir Rudra ^{1*}

Ritabrata Biswas ^{2†}

Ujjal Debnath ^{3*}

**Department of Mathematics, Bengal Engineering and Science University, Shibpur, Howrah-711 103, India.*

† Department of Physics, Indian Institute of Science, Bangalore, India.

Pacs no : 04.20 -q, 04.40 Dg, 97.10. Cv.

Abstract

In this work the collapsing process of a spherically symmetric star, made of dust cloud, in the background of dark energy is studied for two different gravity theories separately, i.e., DGP Brane gravity and Loop Quantum gravity. Two types of dark energy fluids, namely, Modified Chaplygin gas and Generalised Cosmic Chaplygin gas are considered for each model. Graphs are drawn to characterize the nature and the probable outcome of gravitational collapse. A comparative study is done between the collapsing process in the two different gravity theories. It is found that in case of dark matter, there is a great possibility of collapse and consequent formation of Black hole. In case of dark energy possibility of collapse is far lesser compared to the other cases, due to the large negative pressure of dark energy component. There is an increase in mass of the cloud in case of dark matter collapse due to matter accumulation. The mass decreases considerably in case of dark energy due to dark energy accretion on the cloud. In case of collapse with a combination of dark energy and dark matter, it is found that in the absence of interaction there is a far better possibility of formation of black hole in DGP brane model compared to Loop quantum cosmology model.

¹prudra.math@gmail.com

²ritabrata@phys.iisc.ernet.in, biswas.ritabrata@gmail.com

³ujjal@iucaa.ernet.in, ujjaldebnath@yahoo.com

Contents

1	Introduction	2
2	General Formulation of the Collapsing process	3
3	Gravitational Collapse in DGP brane Scenario	4
3.1	Collapse with Dark Matter	4
3.2	Collapse with Dark Energy in the form of Modified Chaplygin gas	6
3.3	Collapse with Dark Energy in the form of Generalised Cosmic Chaplygin Gas	7
3.4	Effect of a combination of dark matter and dark energy(in the form of MCG)	8
3.4.1	Case I : $Q = 0$ i.e., No Interaction Between Dark Matter And Dark Energy:	8
3.4.2	Case II : $Q \neq 0$ i.e., Interaction Between Dark Matter And Dark Energy:	10
3.5	Effect of combination of dark matter and dark energy(in the form of GCCG)	11
3.5.1	Case I : $Q = 0$ i.e., No Interaction Between Dark Matter And Dark Energy:	11
3.5.2	Case II : $Q \neq 0$ i.e., Interaction Between Dark Matter And Dark Energy:	13
4	Gravitational Collapse in Loop Quantum Cosmology	14
4.1	Collapse with Dark Matter	15
4.2	Collapse with Dark Energy in the form of Modified Chaplygin gas	15
4.3	Collapse with Dark Energy in the form of Generalised Cosmic Chaplygin Gas	17
4.4	Effect of combination of Dark Energy(in the form of MCG) and Dark Matter	18
4.4.1	Case I : $Q = 0$ i.e., No Interaction Between Dark Matter And Dark Energy:	18
4.4.2	Case II : $Q \neq 0$ i.e., Interaction Between Dark Matter And Dark Energy:	20
4.5	Effect of combination of Dark Energy(in the form of GCCG) and Dark Matter	20
4.5.1	Case I : $Q = 0$ i.e., Non-Interaction Between Dark Matter And Dark Energy:	20
4.5.2	Case II : $Q \neq 0$ i.e., Interaction Between Dark Matter And Dark Energy:	22
5	Detailed Graphical Analysis	22
6	Discussions and Concluding Remarks	23

1 Introduction

The most remarkable and significant discovery in recent past in the field of cosmology is the discovery of the fact, that our universe is undergoing an accelerated expansion of late [1, 2]. This event has overturned a few stones in the traditional theories of cosmology. Einstein’s equation needed serious revisions in order to account for the observed cosmic acceleration.

Some cosmologists succeeded in affecting proper revisions to the Einstein’s equation by introducing changes in the right side, i.e., introducing the concept of Dark Energy (DE hereafter)[3] component with negative pressure which is responsible for the accelerated expansion of the universe. There have been a lot of research on DE till date. Many candidates having the potential to play the role of DE have surfaced. Among them the DE associated with a scalar field is often called quintessence. In the cosmological context Chaplygin gas was first suggested as an alternative to quintessence. The earliest form of this was known as Pure Chaplygin gas [4, 5]. Gradually Generalized Chaplygin gas [6, 7, 8] was formulated and finally Modified Chaplygin Gas (MCG) came to the foreground. The equation of state followed by MCG [9, 10] is given by

$$p = A\rho_{MCG} - \frac{B}{\rho_{MCG}^\alpha}, \tag{1}$$

where p and ρ are respectively the pressure and energy density and $0 \leq \alpha \leq 1$, and $A, B > 0$. MCG appears to be consistent with the WMAP 5-year data and henceforth support the unified model with DE and dark matter(DM) based on generalized Chaplygin gas [11, 12, 13, 14, 15]. MCG demonstrates an increasing Λ behaviour for the evolution of the universe [4]. Recent developments regarding MCG can be found in [16, 17, 18, 19]. Recent supernovae data also favors the two-fluid cosmological model with Chaplygin gas and matter [20].

In this paper in addition to MCG we will study the gravitational collapse of a star in presence of one more fluid known as, Generalized Cosmic Chaplygin Gas(GCCG). Pedro F. Gonzalez-Diaz [21] for the first time presented the idea of GCCG. His main motivation was to study DE accretion onto Black Hole(BH), and by using GCCG as DE he showed that Big Rip, i.e., singularity at a finite time, is completely out of question, which was an essential component of the previous models. The Equation of state for GCCG is given by,

$$p = -\rho_{GCCG}^{-\alpha} \left[C' + (\rho_{GCCG}^{1+\alpha} - C')^{-\omega} \right] \quad (2)$$

where $C' = \frac{A'}{1+\omega} - 1$. Here A' is a constant which can take on both positive and negative values, and $0 > \omega > -\mathcal{L}$, \mathcal{L} being a positive definite constant which can take on values larger than unity. GCCG can explain the evolution of universe starting from dust era to Λ CDM, radiation era, matter dominated quintessence and lastly phantom era [22].

It is a known that general relativity is incomplete as a theory of gravity. The reason being that the gravitational collapse of physical matter produces a BH with a singularity inside, which is a point in space-time where the curvature and energy density diverge. At this point all mathematical structures break down preventing any further analysis beyond the singularity. Herein lies the motivation for extensive research in gravitational collapse. Till date a lot of significant work has been done in gravitational collapse starting from the pioneering works of Oppenheimer and Snyder [23]. In this paper our motivation is to study the nature and outcome of gravitational collapse of a star made up of DM in the background of DE (of different forms), in two types of widely known gravity theories.

The paper is organized as follows: In section 2, the general formulation of the collapsing process of a cloud is given. Section 3 and section 4 deals with the details of collapsing procedure in DGP brane model and Loop quantum cosmology(LQC) respectively. Finally the paper ends with some concluding remarks in section 6.

2 General Formulation of the Collapsing process

The flat, homogeneous and isotropic FRW model of the universe is described by the line element

$$ds^2 = dt^2 + a^2(t) [dr^2 + r^2 (d\theta^2 + \text{Sin}^2\theta d\phi^2)] \quad (3)$$

The energy conservation equation is given by

$$\dot{\rho}_T + 3\frac{\dot{a}}{a}(\rho_T + p_T) = 0 \quad (4)$$

with $\rho_T = \rho_M + \rho_E$ and $p_T = p_M + p_E$.

The interaction $Q(t)$ between DM and DE can be expressed as

$$\dot{\rho}_M + 3\frac{\dot{a}}{a}\rho_M = Q \quad (5)$$

$$\dot{\rho}_E + 3\frac{\dot{a}}{a}(\rho_E + p_E) = -Q \quad (6)$$

Now, if we consider gravitational collapse of a spherical cloud consists of above DM and DE distribution and is bounded by the surface $\Sigma : r = r_\Sigma$ then the metric on it can be written as

$$ds^2 = dT^2 - R^2(T)\{d\theta^2 + \text{Sin}^2\theta d\phi^2\} \quad (7)$$

Thus on $\Sigma : T = t$ and $R(T) = r_\Sigma a(T)$ where $R(r, t) \equiv ra(t)$ is the geometrical radius of the two spheres $t, r = \text{constant}$. Also the total mass of the collapsing cloud is given by

$$M(T) = m(r, t)|_{r=r_\Sigma} = \frac{1}{2}r^3 a \dot{a}^2 \Big|_\Sigma = \frac{1}{2}R(T)\dot{R}^2(T) \quad (8)$$

The apparent horizon is defined as

$$R_{,\alpha} R_{,\beta} g^{\alpha\beta} = 0, \quad i.e., \quad r^2 \dot{a}^2 = 1 \quad (9)$$

So if $T = T_{AH}$ be the time when the whole cloud starts to be trapped then

$$\dot{R}^2(T_{AH})\Big|_{\Sigma} = r_{\Sigma}^2 \dot{a}^2(T_{AH}) = 1 \quad (10)$$

As it is usually assumed that the collapsing process starts from regular initial data so initially at $t = t_i (< T_{AH})$, the cloud is not trapped i.e.,

$$r_{\Sigma}^2 \dot{a}^2(t_i) < 1, \quad (r_{\Sigma} \dot{a}(t_i) > -1) \quad (11)$$

Thus if equation (10) has any real solution for T_{AH} satisfying (11) then black hole(BH) will form, otherwise the collapsing process leads to a naked singularity(NS). So the gravitational collapse and consequently the formation of a BH solely depends upon the nature of root obtained from equation (10). If any real solution for T_{AH} exists for equation (10) then apparent horizon will be formed and thus a BH. If there is no real solution the collapse is destined to result in a NS.

3 Gravitational Collapse in DGP brane Scenario

A simple and effective model of brane-gravity is the Dvali-Gabadadze-Porrati (DGP) braneworld model [24, 25, 26] which models our 4-dimensional world as a FRW brane embedded in a 5-dimensional Minkowski bulk. It explains the origin of DE as the gravity on the brane leaking to the bulk at large scale. On the 4-dimensional brane the action of gravity is proportional to M_p^2 whereas in the bulk it is proportional to the corresponding quantity in 5-dimensions. The model is then characterized by a cross over length scale $r_c = \frac{M_p^2}{2M_5^2}$ such that gravity is 4-dimensional theory at scales $a \ll r_c$ where matter behaves as pressureless dust, but gravity leaks out into the bulk at scales $a \gg r_c$ and matter approaches the behaviour of a cosmological constant. Moreover it has been shown that the standard Friedmann cosmology can be firmly embedded in DGP brane.

The Friedmann equation in DGP brane model is modified to the equation

$$H^2 = \left(\sqrt{\frac{\rho_T}{3} + \frac{1}{4r_c^2}} + \epsilon \frac{1}{2r_c} \right)^2 \quad (12)$$

and

$$\left(2H - \frac{\epsilon}{r_c} \right) \dot{H} = -H (\rho_T + p_T), \quad (13)$$

where $H = \frac{\dot{a}}{a}$ is the Hubble parameter, ρ_T and p_T are the total cosmic fluid energy density and pressure respectively and $r_c = \frac{M_p^2}{2M_5^2}$ is the cross-over scale which determines the transition from 4D to 5D behaviour and $\epsilon = \pm 1$ (choosing $M_p^2 = 8\pi G = 1$). For $\epsilon = +1$, we have standard DGP(+) model which is self accelerating model without any form of DE, and effective w is always non-phantom. However for $\epsilon = -1$, we have DGP(-) model which does not self accelerate but requires DE on the brane.

In this section the role of DM and DE will be shown separately during the collapse. Then we will study the effect of the combination of DE and DM in the collapsing process, both in the presence and in the absence of interaction.

3.1 Collapse with Dark Matter

Here $\rho_M \neq 0$, $\rho_E = p_E = 0$. So from conservation equation (5), we have

$$\rho_M = \frac{C_0}{a^3} \quad (14)$$

where C_0 is the constant of integration. Using this relation in equation (12) we get, for DGP(+) model: i.e., for $\epsilon = +1$

$$\frac{2}{3\alpha} \left[\frac{\sqrt{\alpha + a^3}}{2} a^{\frac{3}{2}} + \frac{\alpha}{2} \log \left(a^{\frac{3}{2}} + \sqrt{\alpha + a^3} \right) - \frac{a^3}{2} \right] = -\frac{t}{2r_c} + D_0 \quad (15)$$

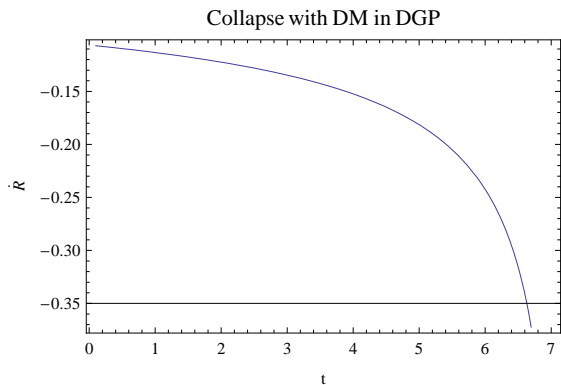


Fig. 1

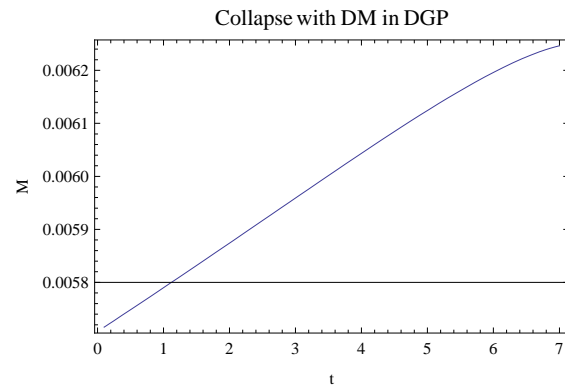


Fig. 2

Fig 1 : The time derivative of the radius is plotted against time. $\alpha = 0.5$, $r = 10$, $r_c = 100$ is considered.

Fig 2 : The mass of the collapsing cloud is plotted against time. $\alpha = 0.5$, $r = 10$, $r_c = 100$ is considered.

The corresponding expression for DGP(-) model: i.e., for $\epsilon = -1$ is,

$$\frac{2}{3\alpha} \left[\frac{\sqrt{\alpha + a^3}}{2} a^{\frac{3}{2}} + \frac{\alpha}{2} \log \left(a^{\frac{3}{2}} + \sqrt{\alpha + a^3} \right) + \frac{a^3}{2} \right] = -\frac{t}{2r_c} + D_0 \quad (16)$$

Where D_0 is the integration constant and $\alpha = \frac{4r_c^2 C_0}{3}$, Considering DGP(-) model and using the value of ρ_M from equation(14) and using the relation $\rho_T = \rho_M + \rho_E$, the expressions for the time derivative of geometrical radius \dot{R} and mass $M(T)$ of the collapsing object are obtained as follows,

$$\dot{R}(T) = -\frac{r_\Sigma (\sqrt{\alpha + a^3} - a^{3/2})}{2\sqrt{a} r_c} \quad (17)$$

and

$$M(T) = \frac{r_\Sigma^3 (\sqrt{\alpha + a^3} - a^{3/2})^2}{8r_c^2} \quad (18)$$

From the above solutions it is evident that as $T \rightarrow \infty$, $a \rightarrow \infty$, $\rho_M \rightarrow 0$, $\dot{R} \rightarrow 0$, $M(T) \rightarrow 0$. So we see that there is a tendency of matter density being diminished as time passes, and finally it tends towards zero. The time for formation of apparent horizon is given by the real root of the equation, $\dot{R}^2(T_{AH})|_\Sigma = r_\Sigma^2 \dot{a}^2(T_{AH}) = 1$ as given by equation (10). Thus the corresponding expression for DGP brane is,

$$r_\Sigma^2 \left(\sqrt{\alpha + a^3} - a^{3/2} \right)^2 = 4ar_c^2 \quad (19)$$

The cloud initially starts untrapped, and gradually as T becomes equal to T_{AH} , the apparent horizon starts forming and the cloud begins to be shrouded by the horizon. The result is the formation of a BH singularity.

Normal collapse of matter influences every collapsing particle to move towards the collapsing centre. So for a normal matter it is quite natural to have a negative outward velocity at a particular point. With time as the collapse centre gathers more mass, the increasing gravitational attraction pulls the rest particles more efficiently causing an increasing negative outward velocity. The same here seems to happen for the case of DM. As we do not have any previous idea of the time gradient of DM collapse. So we cannot comment whether this is normal or something different.

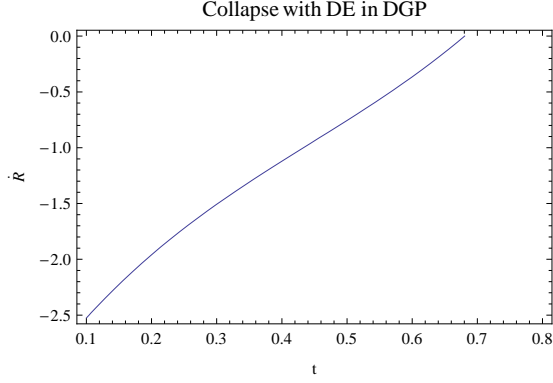


Fig. 3

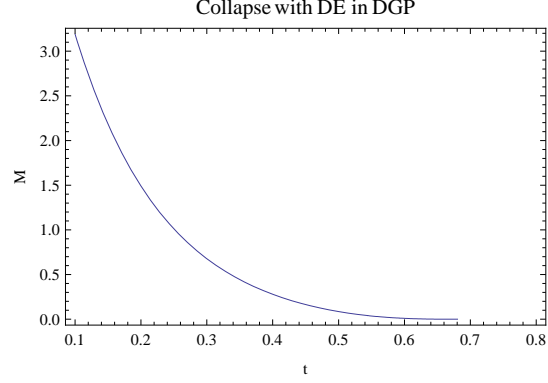


Fig. 4

Fig 3 : The time derivative of the radius is plotted against time. $r = 10$, $r_c = 1000$, $C_1 = 0.05$, $X_1 = 40$, $X_2 = 0.04$, $X_3 = 0.4$ is considered.

Fig 4 : The mass of the collapsing cloud is plotted against time. $r = 10$, $r_c = 1000$, $C_1 = 0.05$, $X_1 = 40$, $X_2 = 0.04$, $X_3 = 0.4$ is considered.

3.2 Collapse with Dark Energy in the form of Modified Chaplygin gas

DE in the form of MCG is considered in this section. Here, $\rho_M = 0$, $p_{MCG} = A\rho_{MCG} - \frac{B}{\rho_{MCG}^\alpha}$. So the solution for density is given by

$$\rho_{MCG} = \left[\frac{B}{1+A} + \frac{C_1}{a^{3(1+A)(1+\alpha)}} \right]^{\frac{1}{1+\alpha}} \quad (20)$$

The expressions for relevant physical quantities are

$$\dot{R}(T) = -r_\Sigma a \left[\sqrt{\frac{1}{3} \left(X_1 + \frac{C_1}{a^{X_2}} \right)^{2X_3} + \frac{1}{4r_c^2} + \frac{\epsilon}{2r_c}} \right] \quad (21)$$

and

$$M(T) = \frac{1}{2} r_\Sigma^3 a^3 \left[\sqrt{\frac{1}{3} \left(X_1 + \frac{C_1}{a^{X_2}} \right)^{2X_3} + \frac{1}{4r_c^2} + \frac{\epsilon}{2r_c}} \right]^2 \quad (22)$$

where $X_1 = \frac{B}{1+A}$, $X_2 = 3(1+A)(1+\alpha)$, $X_3 = \frac{1}{2(1+\alpha)}$. The limiting values of the physical parameters are as follows:

case1

$$a \rightarrow 0: \quad \rho_{MCG} \rightarrow \infty, \quad \text{for } 1+A > 0; \quad \rho_{MCG} \rightarrow \left[\frac{B}{1+A} \right]^{\frac{1}{1+\alpha}}, \quad \text{for } 1+A < 0$$

$$\dot{R} \rightarrow \frac{-rC_1^{\frac{1}{2(1+\alpha)}} a^{\frac{-(1+3A)}{2}}}{\sqrt{3}r_c}, \quad \text{for } 1+A > 0; \quad \dot{R} \rightarrow -\infty, \quad \text{for } 1+A < 0$$

$$M(T) \rightarrow \frac{r^3 a^{-3A} C_1^{\frac{1}{1+\alpha}}}{6}, \quad \text{for } 1+A > 0; \quad M(T) \rightarrow \infty, \quad \text{for } 1+A < 0$$

case2

$$a \rightarrow \infty: \quad \rho_{MCG} \rightarrow \left[\frac{B}{1+A} \right]^{\frac{1}{1+\alpha}}, \quad \text{for } 1+A > 0; \quad \rho_{MCG} \rightarrow \infty, \quad \text{for } 1+A < 0$$

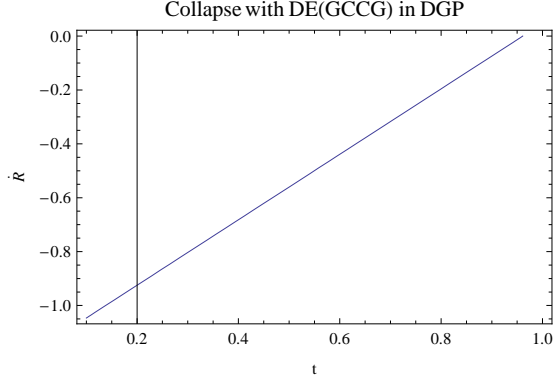


Fig. 5

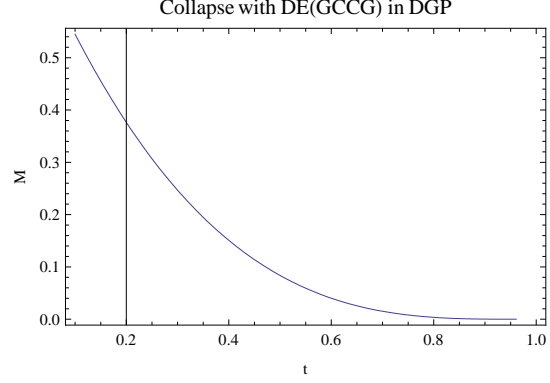


Fig. 6

Fig 5 : The time derivative of the radius is plotted against time. $r = 10$, $r_c = 100000$, $C' = 10$, $B' = 5$, $X_1 = 0.00005$, $X_2 = 1.5$, $X_3 = 0.25$ is considered.

Fig 6 : The mass of the collapsing cloud is plotted against time. $r = 10$, $r_c = 100000$, $C' = 10$, $B' = 5$, $X_1 = 0.00005$, $X_2 = 1.5$, $X_3 = 0.25$ is considered.

$$\dot{R} \rightarrow -\infty, \quad \text{for } 1 + A > 0; \quad \dot{R} \rightarrow \frac{-rC_1^{\frac{1}{2(1+\alpha)}} a^{\frac{-(1+3A)}{2}}}{\sqrt{3r_c}}, \quad \text{for } 1 + A < 0$$

$$M(T) \rightarrow \infty, \quad \text{for } 1 + A > 0; \quad M(T) \rightarrow \frac{r^3 a^{-3A} C_1^{\frac{1}{1+\alpha}}}{6}, \quad \text{for } 1 + A < 0$$

The limiting value of $M(T)$ for $1 + A > 0$ is unphysical for $a \rightarrow \infty$. This is because the mass of the collapsing cloud has to decrease in presence of MCG due to accretion. The cloud will start untrapped at the instant given by the real roots of the following equation and gradually start to be trapped,

$$r_\Sigma^2 a^2 \left[\sqrt{\frac{1}{3} \left(X_1 + \frac{C_1}{a^{X_2}} \right)^{2X_3} + \frac{1}{4r_c^2} + \frac{\epsilon}{2r_c}} \right]^2 = 1 \quad (23)$$

In Fig.3 and Fig.4 we find the time gradient for R, i.e., \dot{R} and mass against time for DE collapse. Here we can see that at first the DE collapse requires an outward negative velocity. However, \dot{R} has a monotonically decreasing magnitude which tends to zero with increasing time. This implies, with time the DE collapse decreases, the tendency to collapse. Even the final fate might be the fact that there is no ingoing fluid. The change of mass is quite amazing in nature as it sharply indicates that matter is flowing outward from collapsing centre.

3.3 Collapse with Dark Energy in the form of Generalised Cosmic Chaplygin Gas

Here DE in the form of GCCG is considered. So, $\rho_M = 0$, $p = -\rho_{GCCG}^{-\alpha} \left[C' + (\rho_{GCCG}^{1+\alpha} - C')^{-\omega} \right]$ as given in equation (2). The solution for density is given by

$$\rho_{GCCG} = \left[C' + \left\{ 1 + \frac{B'}{a^{3(1+\alpha)(1+\omega)}} \right\}^{\frac{1}{1+\omega}} \right]^{\frac{1}{1+\alpha}}, \quad B' \text{ is positive integration constant.} \quad (24)$$

The expressions for relevant physical quantities are

$$\dot{R}(T) = -r_\Sigma a \left[\sqrt{\frac{1}{3} \left[C' + \left\{ 1 + \frac{B'}{a^{X_2'}} \right\}^{X_1'} \right]^{2X_3'} + \frac{1}{4r_c^2} + \frac{\epsilon}{2r_c}} \right] \quad (25)$$

and

$$M(T) = \frac{1}{2} r_{\Sigma}^3 a^3 \left[\sqrt{\frac{1}{3} \left[C' + \left\{ 1 + \frac{B'}{a^{X'_2}} \right\}^{X'_1} \right]^{2X'_3} + \frac{1}{4r_c^2} + \frac{\epsilon}{2r_c}} \right]^2 \quad (26)$$

where $X'_1 = \frac{1}{1+\omega}$, $X'_2 = 3(1+\alpha)(1+\omega)$, $X'_3 = \frac{1}{2(1+\alpha)}$. The limiting values of the physical parameters are as follows:

case1

$$\begin{aligned} a \rightarrow 0: \quad \rho_{GCCG} &\rightarrow \infty, \quad \text{for } 1+\omega > 0; \quad \rho_{GCCG} \rightarrow (C'+1)^{\frac{1}{1+\alpha}}, \quad \text{for } 1+\omega < 0 \\ \dot{R} &\rightarrow -\frac{r}{\sqrt{3}a} B'^{\frac{1}{2(1+\alpha)(1+\omega)}}, \quad \text{for } 1+\omega > 0 \\ M(T) &\rightarrow \frac{r^3}{6a^2} B'^{\frac{1}{(1+\alpha)(1+\omega)}}, \quad \text{for } 1+\omega > 0 \end{aligned}$$

case2

$$\begin{aligned} a \rightarrow \infty: \quad \rho_{GCCG} &\rightarrow \infty, \quad \text{for } 1+\omega < 0; \quad \rho_{GCCG} \rightarrow (C'+1)^{\frac{1}{1+\alpha}}, \quad \text{for } 1+\omega > 0 \\ \dot{R} &\rightarrow -\frac{ra}{2\sqrt{3}r_c} \left(\sqrt{4r_c^2 C'^{\frac{1}{1+\alpha}} + 3} + \sqrt{3}\epsilon \right), \quad \text{for } 1+\omega > 0 \\ M(T) &\rightarrow \frac{ar^3}{24r_c^2} \left(\sqrt{4r_c^2 (C'+1)^{\frac{1}{1+\alpha}} + 3} + \sqrt{3}\epsilon \right)^2, \quad \text{for } 1+\omega > 0 \end{aligned}$$

The corresponding expression for the formation of event horizon is,

$$r_{\Sigma}^2 a^2 \left[\sqrt{\frac{1}{3} \left[C' + \left\{ 1 + \frac{B'}{a^{X'_2}} \right\}^{X'_1} \right]^{2X'_3} + \frac{1}{4r_c^2} + \frac{\epsilon}{2r_c}} \right]^2 = 1 \quad (27)$$

Fig.5 and Fig.6 are the graphs for \dot{R} and M respectively for GCCG collapse. They almost resemble with Fig.3 and Fig.4 respectively. Only the \dot{R} curve is almost a straight line whereas in case of MCG, it was a curved one.

3.4 Effect of a combination of dark matter and dark energy(in the form of MCG)

3.4.1 Case I : $Q = 0$ i.e., No Interaction Between Dark Matter And Dark Energy:

Energy density of matter as given by equation (14) is $\rho_M = \frac{C_0}{a^3}$. Also the energy density of MCG is given in equation (20). The expressions for relevant physical quantities are

$$\dot{R}(T) = -r_{\Sigma} a \left[\sqrt{\frac{1}{3} \left\{ \frac{C_0}{a^3} + \left(X_1 + \frac{C_1}{a^{X_2}} \right)^{2X_3} \right\}} + \frac{1}{4r_c^2} + \frac{\epsilon}{2r_c} \right] \quad (28)$$

and

$$M(T) = \frac{1}{2} r_{\Sigma}^3 a^3 \left[\sqrt{\frac{1}{3} \left\{ \frac{C_0}{a^3} + \left(X_1 + \frac{C_1}{a^{X_2}} \right)^{2X_3} \right\}} + \frac{1}{4r_c^2} + \frac{\epsilon}{2r_c} \right]^2 \quad (29)$$

The limiting values of the physical parameters are as follows,

case1

$$a \rightarrow 0: \quad \rho_M \rightarrow \infty, \quad \rho_{MCG} \rightarrow \infty, \quad \text{for } 1+A > 0; \quad \rho_{MCG} \rightarrow \left[\frac{B}{1+A} \right]^{\frac{1}{1+\alpha}}, \quad \text{for } 1+A < 0$$

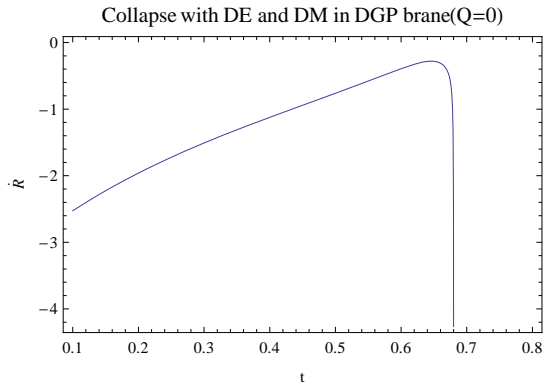


Fig. 7

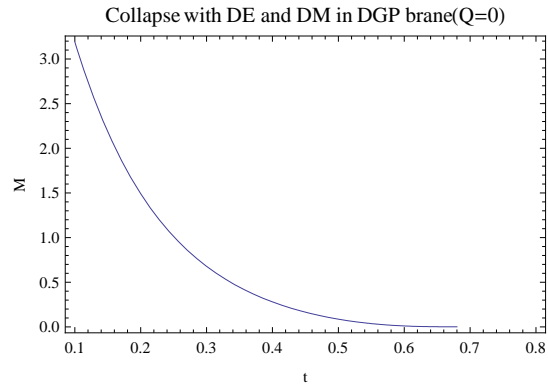


Fig. 8

Fig 7 : The time derivative of the radius is plotted against time. $r = 10$, $r_c = 1000$, $C_0 = 0.00001$, $C_1 = 0.05$, $X_1 = 40$, $X_2 = 0.04$, $X_3 = 0.4$ is considered.

Fig 8 : The mass of the collapsing cloud is plotted against time. $r = 10$, $r_c = 1000$, $C_0 = 0.00001$, $C_1 = 0.05$, $X_1 = 40$, $X_2 = 0.04$, $X_3 = 0.4$ is considered.

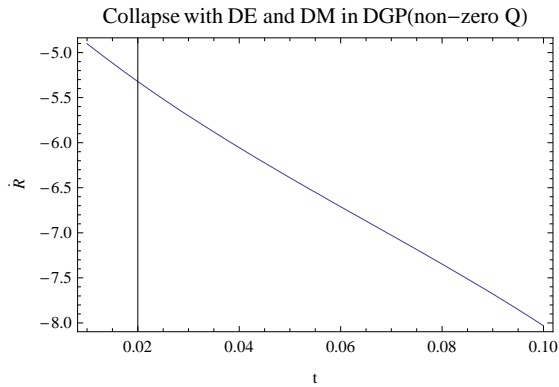


Fig. 9

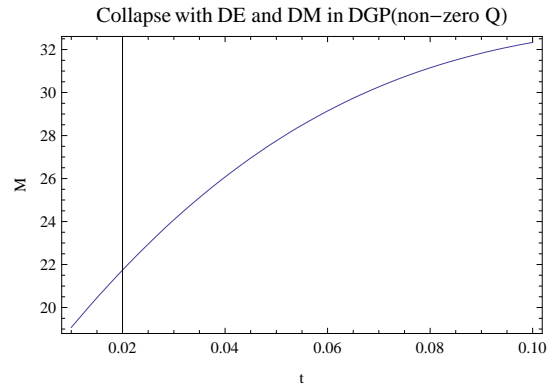


Fig. 10

Fig 9 : The time derivative of the radius is plotted against time. $r = 10$, $r_c = 1000$, $n = 1$, $A = 1$, $B = 1000$, $\alpha = 0.5$, $z_0 = 1$ is considered.

Fig 10 : The mass of the collapsing cloud is plotted against time. $r = 10$, $r_c = 1000$, $n = 1$, $A = 1$, $B = 1000$, $\alpha = 0.5$, $z_0 = 1$ is considered.

$$\dot{R} \rightarrow \frac{-\epsilon ar}{2r_c}, \quad \text{for } 1+A > 0; \quad M(T) \rightarrow \frac{C_1^{\frac{1}{1+\alpha}} a^{-3A} r^3}{6}, \quad \text{for } 1+A > 0$$

case2

$$a \rightarrow \infty: \quad \rho_M \rightarrow 0, \quad \rho_{MCG} \rightarrow \left[\frac{B}{1+A} \right]^{\frac{1}{1+\alpha}}, \quad \text{for } 1+A > 0; \quad \rho_{MCG} \rightarrow \infty, \quad \text{for } 1+A < 0$$

$$\dot{R} \rightarrow \frac{-\sqrt{2}ra^{-(1+3A)}C_1^{\frac{1}{2(1+\alpha)}}}{3}, \quad \text{for } 1+A < 0; \quad M(T) \rightarrow \frac{C_1^{\frac{1}{1+\alpha}} a^{-3A} r^3}{6}, \quad \text{for } 1+A < 0$$

3.4.2 Case II : $Q \neq 0$ i.e., Interaction Between Dark Matter And Dark Energy:

In this case walking in the path of Cai and Wang [27, 28] we will assume the relation

$$\frac{\rho_{MCG}}{\rho_M} = Ca^{3n} \quad (30)$$

where $C > 0$ and n are arbitrary constants. Now we solve the conservation equations (5) and (6) to get the following expression for ρ_T where $\rho_T = \rho_{MCG} + \rho_M$,

$$\begin{aligned} \rho_T^{\alpha+1} &= \frac{(\alpha+1)B}{[\alpha(n-1)-1]} \frac{(Ca^{3n})^{\frac{2}{n}(\alpha+1-n\alpha)-(\alpha+1)}}{(Ca^{3n}+1)^{\frac{2}{n}(\alpha+1-n\alpha)+A(\alpha+1)}} \\ {}_2F_1 \left[\frac{1+\alpha-n\alpha}{n}, \frac{1+n+\alpha+A+A\alpha}{n}, \frac{1+n+\alpha-n\alpha}{n}, \frac{Ca^{3n}}{1+Ca^{3n}} \right] \\ &+ z_0 \left[Ca^{3n} (1+Ca^{3n})^A \right]^{-(\alpha+1)} \end{aligned} \quad (31)$$

where ${}_2F_1$ is the hypergeometric function and z_0 is the integration constant. Using the relation $\rho_T = \rho_{MCG} + \rho_M$ we get

$$\rho_{MCG} = \frac{Ca^{3n}\rho_T}{1+Ca^{3n}} \quad \rho_M = \frac{\rho_T}{1+Ca^{3n}} \quad (32)$$

The expression for interaction in this case, is obtained by using equations 1, 5 and 12 and is given by,

$$Q = -\frac{3\rho_T}{1+Ca^{3n}} \left[\sqrt{\frac{\rho_T}{3} + \frac{1}{4r_c^2} + \frac{\epsilon}{2r_c}} \right] \left[\frac{1}{1+Ca^{3n}} \left(1 + a^{3n} (C(1+A+3n)) - BC^{-\alpha} a^{-3\alpha n} (1+Ca^{3n})^{\alpha+1} \rho_T^{-\alpha-1} \right) - 1 \right] \quad (33)$$

In this case the value for the gradient of scale factor is given by

$$\begin{aligned} \dot{a} = -a \left[\left(\frac{A_3}{a^{3n}(1+Ca^{3n})^A} \left[\frac{C^{\frac{2}{n}(\alpha+1-n\alpha)} a^{6(\alpha+1-n\alpha)}}{(1+Ca^{3n})^{\frac{2}{n}(\alpha+1-n\alpha)}} {}_2F_1 \left[\frac{1+\alpha-n\alpha}{n}, \frac{1+n+\alpha+A+A\alpha}{n}, \frac{1+n+\alpha-n\alpha}{n}, \right. \right. \right. \\ \left. \left. \left. \frac{Ca^{3n}}{1+Ca^{3n}} \right] + z_1 \right)^{\frac{1}{\alpha+1}} + \frac{1}{4r_c^2} \right)^{\frac{1}{2}} + \frac{\epsilon}{2r_c} \right] \end{aligned} \quad (34)$$

where $A_3 = \frac{1}{3C} \left[\frac{(\alpha+1)B}{\alpha(n-1)-1} \right]^{\frac{1}{1+\alpha}}$, and $z_1 = z_0 \left[\frac{(\alpha+1)B}{\alpha(n-1)-1} \right]^{\frac{-1}{\alpha+1}}$. The corresponding expressions for \dot{R} and mass $M(T)$ is given as follows:

$$\dot{R} = -r_{\Sigma} a \left[\left(\frac{A_3}{a^{3n}(1+Ca^{3n})^A} \left[\frac{C^{\frac{2}{n}(\alpha+1-n\alpha)} a^{6(\alpha+1-n\alpha)}}{(1+Ca^{3n})^{\frac{2}{n}(\alpha+1-n\alpha)}} {}_2F_1 \left[\frac{1+\alpha-n\alpha}{n}, \frac{1+n+\alpha+A+A\alpha}{n}, \frac{1+n+\alpha-n\alpha}{n}, \right. \right. \right. \right.$$

$$\left. \frac{Ca^{3n}}{1+Ca^{3n}} \right] + z_1 \left. \right]^{\frac{1}{\alpha+1}} + \frac{1}{4r_c^2} \left. \right)^{\frac{1}{2}} + \frac{\epsilon}{2r_c} \left. \right] \quad (35)$$

and

$$M(T) = \frac{1}{2}a^3r_\Sigma^3 \left[\left(\frac{A_3}{a^{3n}(1+Ca^{3n})^A} \left[\frac{C^{\frac{2}{n}(\alpha+1-n\alpha)}a^{6(\alpha+1-n\alpha)}}{(1+Ca^{3n})^{\frac{2}{n}(\alpha+1-n\alpha)}} \right. \right. \right. \\ \left. \left. \left. {}_2F_1 \left[\frac{1+\alpha-n\alpha}{n}, \frac{1+n+\alpha+A+A\alpha}{n}, \frac{1+n+\alpha-n\alpha}{n}, \right. \right. \right. \right. \\ \left. \left. \left. \left. \frac{Ca^{3n}}{1+Ca^{3n}} \right] + z_1 \right. \right. \right. \left. \right. \left. \right)^{\frac{1}{\alpha+1}} + \frac{1}{4r_c^2} \left. \right)^{\frac{1}{2}} + \frac{\epsilon}{2r_c} \left. \right]^2 \quad (36)$$

From the above expressions the limiting behaviour of the physical parameters are obtained as follows:

case1

$$a \rightarrow 0 : \quad \rho_M \rightarrow a^{-3n}, \quad \rho_{MCG} \rightarrow a \text{ constant}, \quad \rho_T \rightarrow a^{-3n}, \quad \dot{R} \rightarrow -a^{1-\frac{3n}{2}}, \quad M(T) \rightarrow a^{3(1-n)}$$

case2

$$a \rightarrow \infty : \quad \rho_M \rightarrow a^{-3n(\alpha+1)(A+1)}, \quad \rho_{MCG} \rightarrow a^{-3n(\alpha+1)(A+1)}, \quad \rho_T \rightarrow a^{-3n(\alpha+1)(A+1)}, \quad \dot{R} \rightarrow -a^{1-\frac{3n}{2}(1+A)} \\ M(T) \rightarrow a^{3[1-n(1+A)]}$$

Fig. 7,8,9 and 10 are for the cases where DM and DE are present together. First two characterizes the no interaction scenario, whereas the last two deals with the interaction cases.

When there is no interaction the magnitude of \dot{R} decreases at first followed by a steep increment. This can be interpreted as the domination of DE over DM at the first phase and domination of DM over DE at the latter stage. In either case the mass decreases for no interaction case and lastly becomes asymptotic with time axis.

For interacting DM and DE model, it is clear that DM dominates and the basic nature of the graphs are similar to DM collapse case.

3.5 Effect of combination of dark matter and dark energy(in the form of GCCG)

3.5.1 Case I : $Q = 0$ i.e., No Interaction Between Dark Matter And Dark Energy:

The energy density of DM is given by equation (14) and the energy density of GCCG is given by equation (24). Using these two equations in the modified Friedmann equation for DGP brane, i.e., equation(12), we obtain the expressions for the relevant parameters as given below.

The time derivative of the geometrical radius of the collapsing star is given by,

$$\dot{R}(T) = -ar_\Sigma \left[\sqrt{\frac{1}{3} \left(\frac{C_0}{a^3} + \left(C' + \left(1 + \frac{B'}{a^{X_2}} \right)^{X_1} \right)^{2X_3} \right)} + \frac{1}{4r_c^2} + \frac{\epsilon}{2r_c} \right] \quad (37)$$

The expression for mass of the collapsing cloud is given by,

$$M(T) = \frac{1}{2}a^3r_\Sigma^3 \left[\sqrt{\frac{1}{3} \left(\frac{C_0}{a^3} + \left(C' + \left(1 + \frac{B'}{a^{X_2}} \right)^{X_1} \right)^{2X_3} \right)} + \frac{1}{4r_c^2} + \frac{\epsilon}{2r_c} \right]^2 \quad (38)$$

The limiting values of the physical parameters are given below,

case1

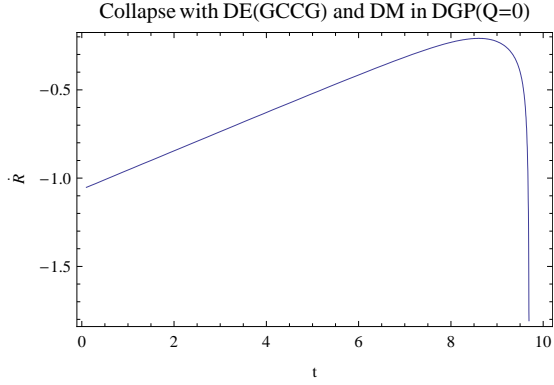


Fig. 11

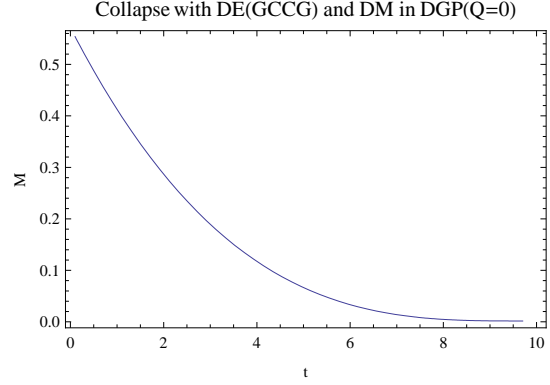


Fig. 12

Fig 11 : The time derivative of the radius is plotted against time. $r = 10$, $r_c = 1000$, $n = 1$, $C' = 10$, $C_0 = 0.00001$, $B' = 5$, $X_1 = 0.00005$, $X_2 = 1.5$, $X_3 = 0.25$ is considered.

Fig 12 : The mass of the collapsing cloud is plotted against time. $r = 10$, $r_c = 1000$, $n = 1$, $C' = 10$, $C_0 = 0.00001$, $B' = 5$, $X_1 = 0.00005$, $X_2 = 1.5$, $X_3 = 0.25$ is considered.

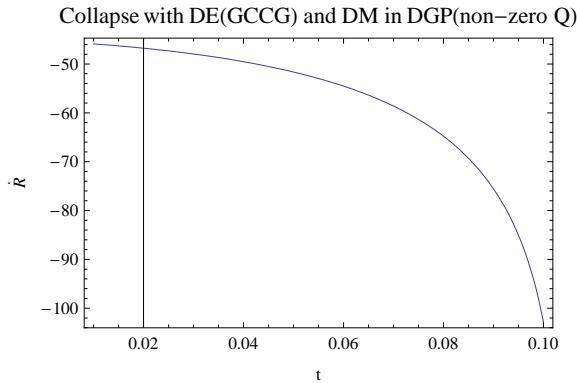


Fig. 13

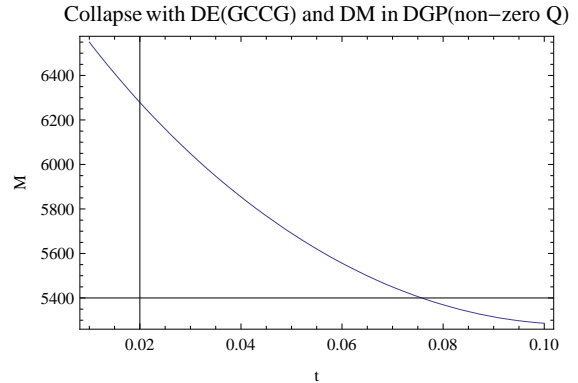


Fig. 14

Fig 13 : The time derivative of the radius is plotted against time. $r = 10$, $r_c = 100000$, $n = 1$, $\tilde{C} = 0.001$, $B' = 5$, $\alpha = 0.5$, $C' = 1000$ is considered.

Fig 14 : The mass of the collapsing cloud is plotted against time. $r = 10$, $r_c = 100000$, $n = 1$, $\tilde{C} = 0.001$, $B' = 5$, $\alpha = 0.5$, $C' = 1000$ is considered.

$$a \rightarrow 0: \quad \rho_{GCCG} \rightarrow \infty, \quad \text{for } 1 + \omega > 0; \quad \rho_{GCCG} \rightarrow (C' + 1)^{\frac{1}{1+\alpha}}, \quad \text{for } 1 + \omega < 0$$

$$\dot{R} \rightarrow -\frac{r}{\sqrt{3a}} \sqrt{C_0 + B'^{\frac{1}{(1+\alpha)(1+\omega)}}}, \quad \text{for } 1 + \omega > 0$$

$$M(T) \rightarrow \frac{r^3}{6} \left(C_0 + B'^{\frac{1}{(1+\alpha)(1+\omega)}} \right), \quad \text{for } 1 + \omega > 0$$

case2

$$a \rightarrow \infty: \quad \rho_{GCCG} \rightarrow \infty, \quad \text{for } 1 + \omega < 0; \quad \rho_{GCCG} \rightarrow (C' + 1)^{\frac{1}{1+\alpha}}, \quad \text{for } 1 + \omega > 0$$

$$\dot{R} \rightarrow -\frac{r\sqrt{a}}{\sqrt{3}} \left[\sqrt{(C' + 1)^{\frac{1}{1+\alpha}} + \frac{3}{4r_c^2} + \frac{\sqrt{3}\epsilon}{2r_c}} \right], \quad \text{for } 1 + \omega > 0$$

$$M(T) \rightarrow \frac{a^3 r^3}{6} \left[\sqrt{(C' + 1)^{\frac{1}{1+\alpha}} + \frac{3}{4r_c^2} + \frac{\sqrt{3}\epsilon}{2r_c}} \right]^2, \quad \text{for } 1 + \omega > 0$$

3.5.2 Case II : $Q \neq 0$ i.e., Interaction Between Dark Matter And Dark Energy:

Like the case of MCG here also we assume the relation

$$\frac{\rho_{GCCG}}{\rho_M} = ka^{3n} \quad (39)$$

where $k > 0$ and n are arbitrary constants. Using this equation and equation 24 in the equations 5 and 6, we calculate the expression for total energy density (ρ_T) as given below,

$$\rho_T = \frac{1}{3a^3} (1 + a^{3n}) \left[9 + \frac{6e^{\tilde{C}}}{1+a} + \frac{12e^{\tilde{C}}}{1-a+a^2} - \frac{6ae^{\tilde{C}}}{1-a+a^2} + \frac{e^{2\tilde{C}}}{(1+a)^2} + \frac{2e^{2\tilde{C}}}{(1+a)} + \frac{3e^{2\tilde{C}}}{(1-a+a^2)^2} \right. \\ \left. - \frac{3ae^{2\tilde{C}}}{(1-a+a^2)^2} + \frac{3e^{2\tilde{C}}}{1-a+a^2} - \frac{2ae^{2\tilde{C}}}{1-a+a^2} + 9C' \right]^{\frac{1}{2}} \quad (40)$$

where \tilde{C} is the integration constant. The above relation is obtained by providing particular values to some of the variables involved in the equation, since the differential equation obtained was not solvable directly. Here the particular values used are $\omega = -\frac{1}{2}$, $k = 1$, $n = 1$ and $\alpha = 1$. Using the relation $\rho_T = \rho_M + \rho_{GCCG}$, we get,

$$\rho_{GCCG} = \frac{ka^{3n}\rho_T}{1+ka^{3n}} \quad \rho_M = \frac{\rho_T}{1+ka^{3n}} \quad (41)$$

The expression for the time derivative of scale factor is given by,

$$\dot{a} = -a \left[\left(\frac{1}{9a^3} (1 + a^{3n}) \left[9 + \frac{6e^{\tilde{C}}}{1+a} + \frac{12e^{\tilde{C}}}{1-a+a^2} - \frac{6ae^{\tilde{C}}}{1-a+a^2} + \frac{e^{2\tilde{C}}}{(1+a)^2} + \frac{2e^{2\tilde{C}}}{(1+a)} + \frac{3e^{2\tilde{C}}}{(1-a+a^2)^2} \right. \right. \right. \\ \left. \left. - \frac{3ae^{2\tilde{C}}}{(1-a+a^2)^2} + \frac{3e^{2\tilde{C}}}{1-a+a^2} - \frac{2ae^{2\tilde{C}}}{1-a+a^2} + 9C' \right]^{\frac{1}{2}} + \frac{1}{4r_c^2} \right)^{\frac{1}{2}} + \frac{\epsilon}{2r_c} \right] \quad (42)$$

The corresponding expressions for other physical parameters are,

$$\dot{R}(T) = -ra \left[\left(\frac{1}{9a^3} (1 + a^{3n}) \left[9 + \frac{6e^{\tilde{C}}}{1+a} + \frac{12e^{\tilde{C}}}{1-a+a^2} - \frac{6ae^{\tilde{C}}}{1-a+a^2} + \frac{e^{2\tilde{C}}}{(1+a)^2} + \frac{2e^{2\tilde{C}}}{(1+a)} + \frac{3e^{2\tilde{C}}}{(1-a+a^2)^2} \right. \right. \right. \\ \left. \left. - \frac{3ae^{2\tilde{C}}}{(1-a+a^2)^2} + \frac{3e^{2\tilde{C}}}{1-a+a^2} - \frac{2ae^{2\tilde{C}}}{1-a+a^2} + 9C' \right]^{\frac{1}{2}} + \frac{1}{4r_c^2} \right)^{\frac{1}{2}} + \frac{\epsilon}{2r_c} \right]$$

$$-\frac{3ae^{2\tilde{C}}}{(1-a+a^2)^2} + \frac{3e^{2\tilde{C}}}{1-a+a^2} - \frac{2ae^{2\tilde{C}}}{1-a+a^2} + 9C' \left. \right]^{\frac{1}{2}} + \frac{1}{4r_c^2} \left. \right)^{\frac{1}{2}} + \frac{\epsilon}{2r_c} \quad (43)$$

and

$$M(T) = \frac{1}{2}a^3r^3 \left[\left(\frac{1}{9a^3} (1+a^{3n}) \left[9 + \frac{6e^{\tilde{C}}}{1+a} + \frac{12e^{\tilde{C}}}{1-a+a^2} - \frac{6ae^{\tilde{C}}}{1-a+a^2} + \frac{e^{2\tilde{C}}}{(1+a)^2} + \frac{2e^{2\tilde{C}}}{(1+a)} + \frac{3e^{2\tilde{C}}}{(1-a+a^2)^2} \right. \right. \right. \\ \left. \left. \left. - \frac{3ae^{2\tilde{C}}}{(1-a+a^2)^2} + \frac{3e^{2\tilde{C}}}{1-a+a^2} - \frac{2ae^{2\tilde{C}}}{1-a+a^2} + 9C' \right]^{\frac{1}{2}} + \frac{1}{4r_c^2} \right)^{\frac{1}{2}} + \frac{\epsilon}{2r_c} \right]^2 \quad (44)$$

Using the conservation equations 5 and 6, and using the expressions for ρ_M , ρ_{GCCG} and ρ_T we get the following expression for the interaction,

$$Q = -\frac{3\rho_T}{1+ka^{3n}} \left[\sqrt{\frac{\rho_T}{3} + \frac{1}{4r_c^2} + \frac{\epsilon}{2r_c}} \right] \left[\frac{1}{1+ka^{3n}} \left(ka^{3n}(n+1) + 1 - k^{-\alpha} \left(\frac{\rho_T}{1+ka^{3n}} \right)^{-(\alpha+1)} a^{-3n\alpha} \right. \right. \\ \left. \left. \left(C' + \left(\left(\frac{ka^{3n}\rho_T}{1+ka^{3n}} \right)^{1+\alpha} - C' \right)^{-\omega} \right) \right) - 1 \right] \quad (45)$$

Fig.11, 12, 13 and 14 are for GCCG case. These are quite similar with figs.7,8,9 and 10 respectively.

4 Gravitational Collapse in Loop Quantum Cosmology

In recent years, loop Quantum Gravity (LQG) is an outstanding effort to describe the quantum effect of our universe [29, 30]. LQG is a theory trying to quantize the gravity with a non-perturbative and background independent method. The theory and principles of LQG when applied in the cosmological framework creates a new theoretical framework of Loop Quantum Cosmology(LQC) [31, 32, 33]. In this theory, classical space-time continuum is replaced by a discrete quantum geometry. The effect of LQG can be described by the modification of Friedmann equation to add a term quadratic in density. In LQC, the non-perturbative effects lead to correction term $\frac{\rho^2}{\rho_1}$ to the standard Friedmann equation. With the inclusion of this term, the universe bounces quantum mechanically as the matter energy density reaches the level of ρ_1 (order of Plank density).

Recently the model of DE has been explored in the framework of LQC. The cosmological evolution in LQC has been widely studied for quintessence and phantom DE models [34]. The modified Friedmann equation for Loop Quantum Cosmology is given by ([35, 36, 37])

$$H^2 = \frac{\rho_T}{3} \left(1 - \frac{\rho_T}{\rho_1} \right) \quad (46)$$

Here $\rho_1 = \sqrt{3}\pi^2\gamma^3G^2\hbar$ is the critical loop quantum density and γ is the dimensionless Barbero-Immirzi parameter. $\rho_T = \rho_M + \rho_E$ represents the total cosmic energy density, which is a sum of energy density of DM (ρ_M) and the energy density of DE (ρ_E).

Like the previous section in this section also we will study the role of DM and DE separately during the collapse. Then we will study the effect of the combination of DE and DM in the collapsing process, both in the presence and in the absence of interaction.

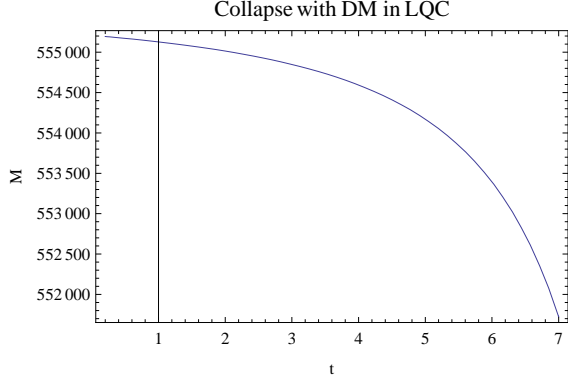


Fig. 15

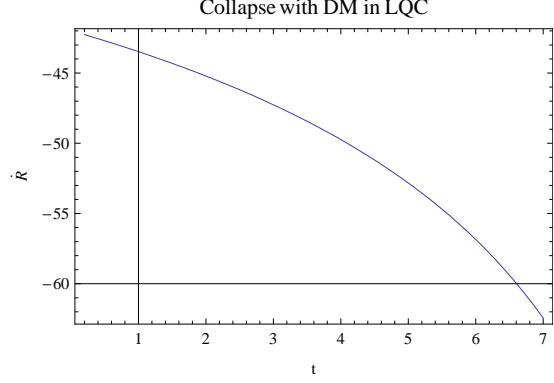


Fig. 16

Fig 15 : The time derivative of the radius is plotted against time. $R_0 = 100$, $n_0 = 0.4$, $N_0 = 0.1$, $T = 10$ is considered.

Fig 16 : The mass of the collapsing cloud is plotted against time. $R_0 = 100$, $n_0 = 0.4$, $N_0 = 0.1$, $T = 10$ is considered.

4.1 Collapse with Dark Matter

Here $\rho_M \neq 0$ and $\rho_E = 0$. From the conservation equations (5) and (6) we get the solution in (14). Putting the obtained value of ρ_M in equation (46) we get

$$a^3 = [n_0 (T_0 - T)]^2 + N_0^2 \quad (47)$$

where $n_0 = \sqrt{\frac{3}{4}C_0}$ and $N_0 = \sqrt{\frac{C_0}{3\rho_1}}$ and T_0 is the integration constant. The time derivative of the geometrical radius of the collapsing object is determined as follows

$$\dot{R}(T) = -\frac{2}{3}R_0 \frac{(a^3 - N_0^2)^{\frac{1}{2}}}{a^2} \quad (48)$$

The total mass of the collapsing cloud as determined is given by

$$M(T) = \frac{2}{9}R_0^3 \frac{(a^3 - N_0^2)}{n_0 a^3}. \quad (49)$$

where $R_0 = r_\Sigma n_0$. The limiting values of the physical parameters are given as $T \rightarrow \infty$, $a \rightarrow \infty$, $\rho_M \rightarrow 0$, $\dot{R} \rightarrow 0$, $M(T) \rightarrow \frac{2R_0^3}{9n_0}$. Like the previous case, the time for formation of apparent horizon is given by the real root of the equation $\dot{R}^2(T_{AH})|_\Sigma = r_\Sigma^2 \dot{a}^2(T_{AH}) = 1$ as given by equation (11). Thus the corresponding expression for LQC is,

$$\left(\frac{4}{9}R_0^2\right)^3 [n_0 (T_0 - T)]^6 = [n_0^2 (T_0 - T)^2 + N_0^2]^4 \quad (50)$$

From the above expression it can be seen that singularity will form at the instant $T = T_0$.

4.2 Collapse with Dark Energy in the form of Modified Chaplygin gas

In this case, $\rho_M = 0$. The expression of the density of MCG as given in equation (20) is $\rho_{MCG} = \left[\frac{B}{1+A} + \frac{C_1}{a^{3(1+A)(1+\alpha)}}\right]^{\frac{1}{1+\alpha}}$. Using this relation in the modified Friedman equation for Loop Quantum Cosmology given in equation (46), we get the expressions for the other relevant physical quantities as follows,

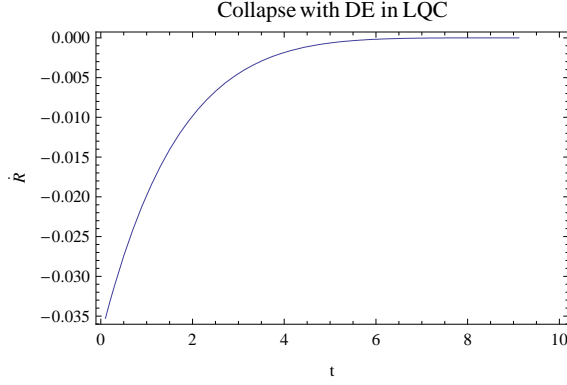


Fig. 17

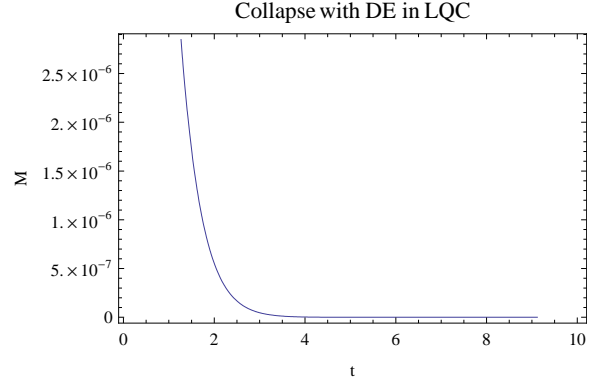


Fig. 18

Fig 17 : The time derivative of the radius is plotted against time. $r = 0.5$, $\rho_1 = 1000$, $C_1 = 0.5$, $X_1 = 0.4$, $X_2 = 0.4$, $X_3 = 0.4$ is considered.

Fig 18 : The mass of the collapsing cloud is plotted against time. $r = 0.5$, $\rho_1 = 1000$, $C_1 = 0.5$, $X_1 = 0.4$, $X_2 = 0.4$, $X_3 = 0.4$ is considered.

$$\dot{R}(T) = -\frac{r_\Sigma a}{\sqrt{3}} \left[X_1 + \frac{C_1}{a^{X_2}} \right]^{X_3} \left[1 - \frac{1}{\rho_1} \left\{ X_1 + \frac{C_1}{a^{X_2}} \right\}^{2X_3} \right]^{\frac{1}{2}} \quad (51)$$

The total mass of the collapsing cloud as determined is given by

$$M(T) = \frac{a^3 r_\Sigma^3}{6} \left[X_1 + \frac{C_1}{a^{X_2}} \right]^{X_3} \left[1 - \frac{1}{\rho_1} \left\{ X_1 + \frac{C_1}{a^{X_2}} \right\}^{2X_3} \right] \quad (52)$$

We know that for the cloud to undergo collapse, we should have $\dot{R} < 0$, and hence from the above expression for \dot{R} , we have

$$a > \frac{C_1^{\frac{1}{X_2}}}{\left(\rho_1^{\frac{1}{2X_3}} - X_1 \right)^{\frac{1}{X_2}}} \quad (53)$$

for $X_2 > 0$, i.e., $1 + A > 0$. Again we should have,

$$a < \left[\frac{1}{C_1} \left(\rho_1^{\frac{1}{2X_3}} - X_1 \right) \right]^{\frac{1}{\mu}} \quad (54)$$

for $X_2 < 0$, i.e., $1 + A < 0$, where $X_2 = -\mu$. The limiting values for the physical parameters are given as follows:

case1

$$a \rightarrow 0: \quad \rho_{MCG} \rightarrow \infty, \quad \text{for } 1 + A > 0; \quad \rho_{MCG} \rightarrow \left[\frac{B}{1 + A} \right]^{\frac{1}{1+A}}, \quad \text{for } 1 + A < 0$$

$$\dot{R}(T) \rightarrow -\frac{r_\Sigma}{\sqrt{3}\rho_1} a^{-(2+3A)} C_1^{2X_3}, \quad \text{for } 1 + A < 0, \quad \text{i.e., } a < \left[\frac{1}{C_1} \left(\rho_1^{\frac{1}{2X_3}} - X_1 \right) \right]^{\frac{1}{\mu}}$$

$$M(T) \rightarrow \frac{r_\Sigma^3}{6\rho_1} C_1^{4X_3} a^{-3(1+2A)}, \quad \text{for } 1 + A < 0$$

case2

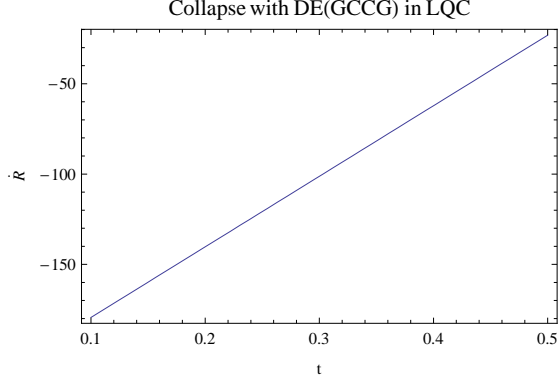


Fig. 19

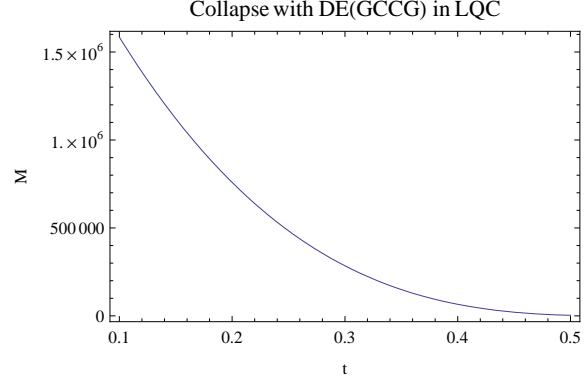


Fig. 20

Fig 19 : The time derivative of the radius is plotted against time. $r = 1000$, $\rho_1 = 1000$, $B' = 5$, $C' = 100$, $X_1 = 0.00005$, $X_2 = 1.5$, $X_3 = 0.25$ is considered.

Fig 20 : The mass of the collapsing cloud is plotted against time. $r = 1000$, $\rho_1 = 1000$, $B' = 5$, $C' = 100$, $X_1 = 0.00005$, $X_2 = 1.5$, $X_3 = 0.25$ is considered.

$$a \rightarrow \infty : \quad \rho_{MCG} \rightarrow \left[\frac{B}{1+A} \right]^{\frac{1}{1+\alpha}}, \quad \text{for } 1+A > 0; \quad \rho_{MCG} \rightarrow \infty, \quad \text{for } 1+A < 0$$

$$\dot{R}(T) \rightarrow -\frac{r_\Sigma}{\sqrt{3}\rho_1} a^{-(2+3A)} C_1^{2X_3}, \quad \text{for } 1+A > 0, \quad \text{i.e., } a > \frac{C_1^{\frac{1}{X_2}}}{\left(\rho_1^{\frac{1}{2X_3}} - X_1 \right)^{\frac{1}{X_2}}}$$

$$M(T) \rightarrow \frac{r_\Sigma^3}{6\rho_1} C_1^{4X_3} a^{-3(1+2A)}, \quad \text{for } 1+A > 0$$

The cloud will start to be trapped at the instant given by the real roots of the equation,

$$\frac{r_\Sigma^2 a^2}{3} \left[X_1 + \frac{C_1}{a^{X_2}} \right]^{2X_3} \left[1 - \frac{1}{\rho_1} \left\{ X_1 + \frac{C_1}{a^{X_2}} \right\}^{2X_3} \right] = 1 \quad (55)$$

4.3 Collapse with Dark Energy in the form of Generalised Cosmic Chaplygin Gas

Here $\rho_M = 0$. The expression for the density of DE is given by equation (24). The expressions for the relevant physical quantities are,

$$\dot{R}(T) = -\frac{ar_\Sigma}{\sqrt{3}} \left[C' + \left(1 + \frac{B'}{a^{X'_2}} \right)^{X'_1} \right]^{X'_3} \left[1 - \frac{1}{\rho_1} \left(C' + \left(1 + \frac{B'}{a^{X'_2}} \right)^{X'_1} \right)^{2X'_3} \right]^{\frac{1}{2}} \quad (56)$$

and

$$M(T) = \frac{a^3 r_\Sigma^3}{6} \left[C' + \left(1 + \frac{B'}{a^{X'_2}} \right)^{X'_1} \right]^{2X'_3} \left[1 - \frac{1}{\rho_1} \left(C' + \left(1 + \frac{B'}{a^{X'_2}} \right)^{X'_1} \right)^{2X'_3} \right] \quad (57)$$

For the cloud to undergo collapse, we should have,

$$a^3 > \frac{1}{\rho_1} \left[C' a^{X'_1 X'_2} + \left(a^{X'_2} + B' \right)^{X'_1} \right]^{2X'_3} \quad (58)$$

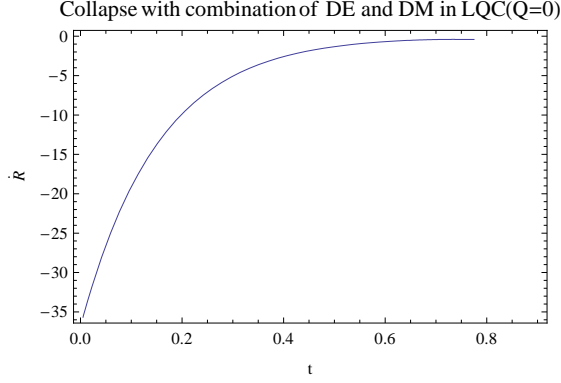


Fig. 21

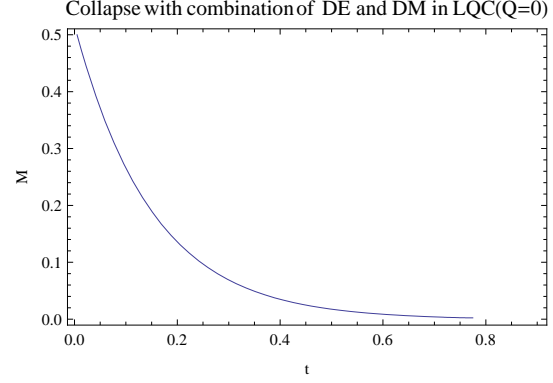


Fig. 22

Fig 21 : The time derivative of the radius is plotted against time. $r = 10$, $\rho_1 = 1000$, $B' = 5$, $C_1 = 500$, $C_0 = 0.00001$, $X_1 = 40$, $X_2 = 0.04$, $X_3 = 0.4$ is considered.

Fig 22 : The mass of the collapsing cloud is plotted against time. $r = 10$, $\rho_1 = 1000$, $B' = 5$, $C_1 = 500$, $C_0 = 0.00001$, $X_1 = 40$, $X_2 = 0.04$, $X_3 = 0.4$ is considered.

The limiting values of the corresponding physical parameters are given as follows,

case1

$$a \rightarrow 0: \quad \rho_{GCCG} \rightarrow \infty, \quad \text{for } 1 + \omega > 0; \quad \rho_{GCCG} \rightarrow [C' + 1]^{\frac{1}{1+\alpha}}, \quad \text{for } 1 + \omega < 0$$

$$\dot{R}(T) \rightarrow -\frac{r_{\Sigma} a^{-2}}{\sqrt{3}\rho_1} B'^{\frac{1}{(1+\alpha)(1+\omega)}}, \quad \text{for } 1 + \omega > 0$$

$$M(T) \rightarrow \frac{r_{\Sigma}^3}{6\sqrt{\rho_1}} B'^{\frac{2}{(1+\alpha)(1+\omega)}}, \quad \text{for } 1 + \omega > 0$$

case2

$$a \rightarrow \infty: \quad \rho_{GCCG} \rightarrow \infty, \quad \text{for } 1 + \omega < 0; \quad \rho_{GCCG} \rightarrow [C' + 1]^{\frac{1}{1+\alpha}}, \quad \text{for } 1 + \omega > 0$$

$$\dot{R}(T) \rightarrow -\frac{r_{\Sigma} a}{\sqrt{3}\rho_1} (C' + 1)^{\frac{1}{2(1+\alpha)}} \left[\rho_1 - (C' + 1)^{\frac{1}{1+\alpha}} \right]^{\frac{1}{2}}, \quad \text{for } 1 + \omega > 0$$

$$M(T) \rightarrow \frac{r_{\Sigma}^3 a^6}{6\sqrt{\rho_1}} (C' + 1)^{\frac{1}{1+\alpha}} \left[\rho_1 - (C' + 1)^{\frac{1}{1+\alpha}} \right], \quad \text{for } 1 + \omega > 0$$

All the above limiting values are calculated considering that equation (58) is satisfied. The time for the formation of the apparent horizon is given by the real root of the following equation,

$$\frac{a^2 r_{\Sigma}^2}{3} \left[C' + \left(1 + \frac{B'}{a^{X_2}} \right)^{X_1'} \right]^{2X_3'} \left[1 - \frac{1}{\rho_1} \left(C' + \left(1 + \frac{B'}{a^{X_2}} \right)^{X_1'} \right)^{2X_3'} \right] = 1 \quad (59)$$

4.4 Effect of combination of Dark Energy(in the form of MCG) and Dark Matter

4.4.1 Case I : $Q = 0$ i.e., No Interaction Between Dark Matter And Dark Energy:

The solution for ρ_M and ρ_{MCG} are given in equations (14) and (20). The relevant physical quantities are obtained as

$$\dot{R}(T) = -\frac{r_{\Sigma} a}{\sqrt{3}} \left[\frac{C_0}{a^3} + \left(X_1 + \frac{C_1}{a^{X_2}} \right)^{2X_3} \right]^{\frac{1}{2}} \left[1 - \frac{1}{\rho_1} \left\{ \frac{C_0}{a^3} + \left(X_1 + \frac{C_1}{a^{X_2}} \right)^{2X_3} \right\} \right]^{\frac{1}{2}} \quad (60)$$

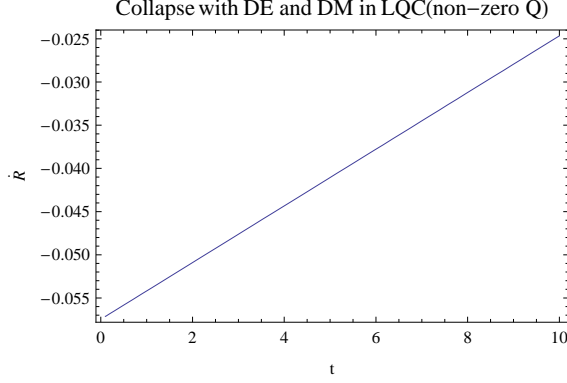


Fig. 23

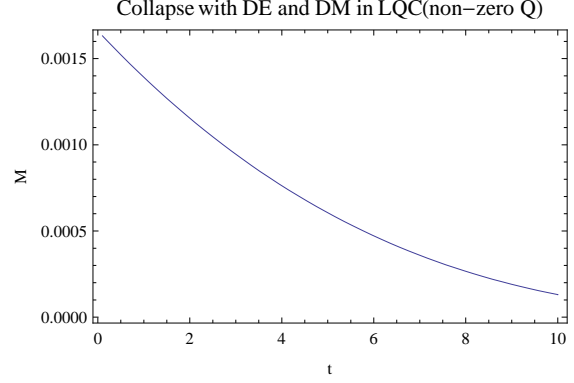


Fig. 24

Fig 23 : The time derivative of the radius is plotted against time. $r = 10$, $\rho_1 = 10$, $B = 5$, $C = 5$, $n = 1$ is considered.

Fig 24 : The mass of the collapsing cloud is plotted against time. $r = 10$, $\rho_1 = 10$, $B = 5$, $C = 5$, $n = 1$ is considered.

and

$$M(T) = \frac{r_\Sigma^3 a^3}{6} \left[\frac{C_0}{a^3} + \left(X_1 + \frac{C_1}{a^{X_2}} \right)^{2X_3} \right] \left[1 - \frac{1}{\rho_1} \left\{ \frac{C_0}{a^3} + \left(X_1 + \frac{C_1}{a^{X_2}} \right)^{2X_3} \right\} \right] \quad (61)$$

In this case, the condition for the cloud to undergo collapse is given by,

$$a^{X_2} \left[\left(\rho_1^2 - \frac{C_0}{a^3} \right)^{\frac{1}{2X_3}} - X_1 \right] > C_1 \quad (62)$$

for $X_2 > 0$, i.e., $1 + A > 0$, and $a \rightarrow \infty$. The above result is also valid for $X_2 < 0$, i.e., $1 + A < 0$, and $a \rightarrow 0$. The limiting values of the physical parameters are as follows,

case1

$$a \rightarrow 0: \quad \rho_M \rightarrow \infty, \quad \rho_{MCG} \rightarrow \infty, \quad \text{for } 1 + A > 0; \quad \rho_{MCG} \rightarrow \left[\frac{B}{1 + A} \right]^{\frac{1}{1+A}}, \quad \text{for } 1 + A < 0$$

$$\dot{R}(T) \rightarrow -\frac{r_\Sigma}{\sqrt{3}\rho_1} a^{-\frac{1}{2}(1+3A)} \left(\frac{C_0}{a^3} + X_1^{2X_3} \right)^{\frac{1}{2}} \left[\rho_1 - \left(\frac{C_0}{a^3} + X_1^{2X_3} \right)^{\frac{1}{2}} \right], \quad \text{for } 1 + A < 0$$

$$M(T) \rightarrow 0, \quad \text{for } 1 + A > 0, \quad M(T) \rightarrow \infty, \quad \text{for } 1 + A < 0$$

case2

$$a \rightarrow \infty: \quad \rho_M \rightarrow 0, \quad \rho_{MCG} \rightarrow \left[\frac{B}{1 + A} \right]^{\frac{1}{1+A}}, \quad \text{for } 1 + A > 0; \quad \rho_{MCG} \rightarrow \infty, \quad \text{for } 1 + A < 0$$

$$\dot{R}(T) \rightarrow -\frac{r_\Sigma}{\sqrt{3}\rho_1} a^{-\frac{1}{2}(1+3A)} \left(\frac{C_0}{a^3} + X_1^{2X_3} \right)^{\frac{1}{2}} \left[\rho_1 - \left(\frac{C_0}{a^3} + X_1^{2X_3} \right)^{\frac{1}{2}} \right], \quad \text{for } 1 + A > 0$$

$$M(T) \rightarrow 0, \quad \text{for } 1 + A < 0, \quad M(T) \rightarrow \infty, \quad \text{for } 1 + A > 0$$

4.4.2 Case II : $Q \neq 0$ i.e., Interaction Between Dark Matter And Dark Energy:

As in the case of DGP brane here also we will assume the relation $\frac{\rho_{MCG}}{\rho_M} = Ca^{3n}$ as given in equation (30). The expressions for ρ_M , ρ_{MCG} and ρ_T are given in equations (14), (24) and (31) respectively. The expression for interaction is given by

$$Q = -\frac{3\rho_T}{1+Ca^{3n}} \left[\sqrt{\frac{\rho_T}{3} \left(1 - \frac{\rho_T}{\rho_1}\right)} \right] \left[\frac{1}{1+Ca^{3n}} \left(1 + a^{3n} (C(1+A+3n)) - BC^{-\alpha} a^{-3\alpha n} (1+Aa^{3n})^{\alpha+1} \rho_T^{-\alpha-1}\right) - 1 \right] \quad (63)$$

In this case the value for the gradient of scale factor is given by

$$\dot{a} = -a \left[\sqrt{\frac{\rho_T}{3} \left(1 - \frac{\rho_T}{\rho_1}\right)} \right] \quad (64)$$

where ρ_T is given by (31). The corresponding expressions for mass $M(T)$ and \dot{R} are given as follows:

$$\dot{R}(T) = -r_\Sigma a \sqrt{\frac{\rho_T}{3} \left(1 - \frac{\rho_T}{\rho_1}\right)} \quad (65)$$

and

$$M(T) = \frac{1}{6} a^3 r_\Sigma^3 \rho_T^2 \left(1 - \frac{\rho_T}{\rho_1}\right) \quad (66)$$

The limiting values for the physical parameters for this case are given by

case1

$$a \rightarrow 0 : \quad \rho_M \rightarrow a^{-3n}, \quad \rho_{MCG} \rightarrow a \text{ constant}, \quad \rho_T \rightarrow a^{-3n}, \quad \dot{R} \rightarrow -a^{1-\frac{3n}{2}}, \quad M(T) \rightarrow a^{3(1-n)}$$

case2

$$a \rightarrow \infty : \quad \rho_M \rightarrow a^{-3n(\alpha+1)(A+1)}, \quad \rho_{MCG} \rightarrow a^{-3n(\alpha+1)(A+1)}, \quad \rho_T \rightarrow a^{-3n(\alpha+1)(A+1)}, \quad \dot{R} \rightarrow -a^{1-\frac{3n}{2}(1+A)}$$

$$M(T) \rightarrow a^{3[1-n(1+A)]}$$

4.5 Effect of combination of Dark Energy(in the form of GCCG) and Dark Matter

4.5.1 Case I : $Q = 0$ i.e., Non-Interaction Between Dark Matter And Dark Energy:

The solution for ρ_M and ρ_{GCCG} are given in equations (14) and (24) respectively. The relevant physical quantities are obtained as

$$\dot{R}(T) = -\frac{ar_\Sigma}{\sqrt{3}} \left[\frac{C_0}{a^3} + \left[C' + \left(1 + \frac{B'}{a^{X_2}}\right)^{X_1'} \right]^{2X_3'} \right]^{\frac{1}{2}} \left[1 - \frac{1}{\rho_1} \left[\frac{C_0}{a^3} + \left(C' + \left(1 + \frac{B'}{a^{X_2}}\right)^{X_1'} \right)^{2X_3'} \right] \right]^{\frac{1}{2}} \quad (67)$$

and

$$M(T) = \frac{a^3 r_\Sigma^3}{6} \left[\frac{C_0}{a^3} + \left[C' + \left(1 + \frac{B'}{a^{X_2}}\right)^{X_1'} \right]^{2X_3'} \right] \left[1 - \frac{1}{\rho_1} \left[\frac{C_0}{a^3} + \left(C' + \left(1 + \frac{B'}{a^{X_2}}\right)^{X_1'} \right)^{2X_3'} \right] \right] \quad (68)$$

The collapsing process will take place provided $\dot{R}(T) < 0$, hence the corresponding condition is given by,

$$a^3 > \frac{1}{\rho_1} \left[C_0 + \left(C' a^{X_1' X_2'} + \left(a^{X_2'} + B' \right)^{X_1'} \right)^{2X_3'} \right] \quad (69)$$

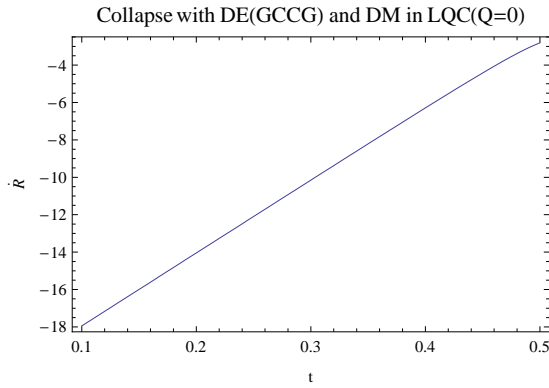


Fig. 25

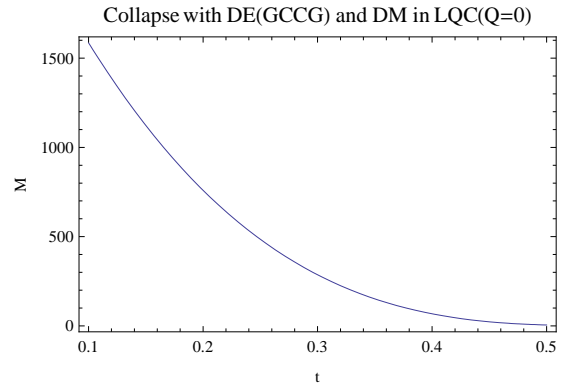


Fig. 26

Fig 25 : The time derivative of the radius is plotted against time. $r = 100$, $\rho_1 = 1000$, $B' = 5$, $C' = 100$, $n = 1$, $X_1 = 0.00005$, $X_2 = 1.5$, $X_3 = 0.25$, $C_0 = 0.00001$ is considered.

Fig 26 : The mass of the collapsing cloud is plotted against time. $r = 100$, $\rho_1 = 1000$, $B' = 5$, $C' = 100$, $n = 1$, $X_1 = 0.00005$, $X_2 = 1.5$, $X_3 = 0.25$, $C_0 = 0.00001$ is considered.

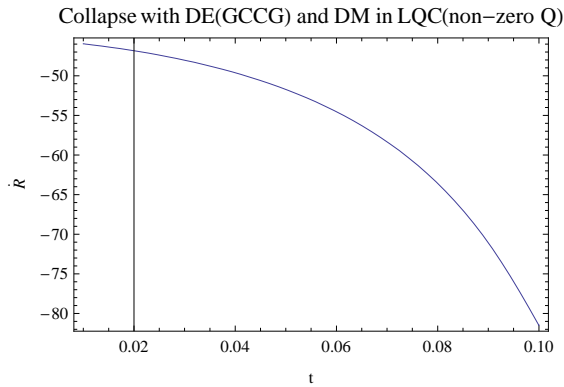


Fig. 27

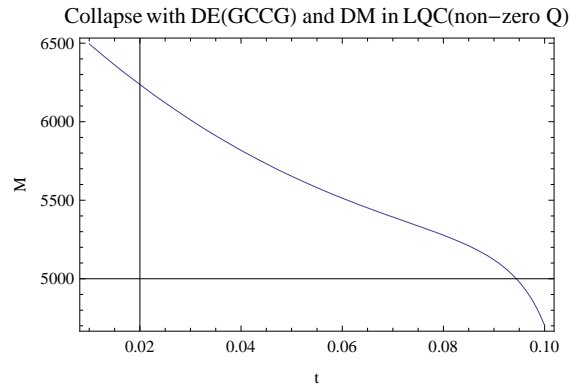


Fig. 28

Fig 27 : The time derivative of the radius is plotted against time. $r = 10$, $\rho_1 = 100000$, $B' = 5$, $\tilde{C} = 0.001$, $n = 1$ is considered.

Fig 28 : The mass of the collapsing cloud is plotted against time. $r = 10$, $\rho_1 = 100000$, $B' = 5$, $\tilde{C} = 0.001$, $n = 1$ is considered.

The corresponding limiting values of different parameters are given below,

case1

$$\begin{aligned}
a \rightarrow 0: \quad \rho_{GCCG} &\rightarrow \infty, \quad \text{for } 1 + \omega > 0; \quad \rho_{GCCG} \rightarrow [C' + 1]^{\frac{1}{1+\alpha}}, \quad \text{for } 1 + \omega < 0 \\
\dot{R}(T) &\rightarrow -\frac{r_{\Sigma} a^{-2}}{\sqrt{3}\rho_1} \left(C_0 + B' \frac{1}{(1+\alpha)(1+\omega)} \right), \quad \text{for } 1 + \omega > 0 \\
M(T) &\rightarrow \frac{r_{\Sigma}^3}{6\sqrt{\rho_1}} \left(C_0 + B' \frac{1}{1+\omega} \right)^{1+\alpha}, \quad \text{for } 1 + \omega > 0
\end{aligned}$$

case2

$$\begin{aligned}
a \rightarrow \infty: \quad \rho_{GCCG} &\rightarrow \infty, \quad \text{for } 1 + \omega < 0; \quad \rho_{GCCG} \rightarrow [C' + 1]^{\frac{1}{1+\alpha}}, \quad \text{for } 1 + \omega > 0 \\
\dot{R}(T) &\rightarrow -\frac{r_{\Sigma} a}{\sqrt{3}\rho_1} (C' + 1)^{\frac{1}{2(1+\alpha)}} \left[\rho_1 - (C' + 1)^{\frac{1}{1+\alpha}} \right]^{\frac{1}{2}}, \quad \text{for } 1 + \omega > 0 \\
M(T) &\rightarrow \frac{r_{\Sigma}^3 a^6}{6\sqrt{\rho_1}} (C' + 1)^{\frac{1}{1+\alpha}} \left[\rho_1 - (C' + 1)^{\frac{1}{1+\alpha}} \right], \quad \text{for } 1 + \omega > 0
\end{aligned}$$

4.5.2 Case II : $Q \neq 0$ i.e., Interaction Between Dark Matter And Dark Energy:

As usual we consider $\frac{\rho_{GCCG}}{\rho_M} = ka^{3n}$, where $k > 0$ and ' n ' is an arbitrary constant. Just like the previous cases the expressions for ρ_M , ρ_{GCCG} and ρ_T are also taken into account from equations (14), (24) and (40) respectively. The relevant parameters, i.e. \dot{a} , $\dot{R}(T)$ and $M(T)$ are given by the equations (64), (65) and (66) respectively using the values of ρ_M , ρ_{GCCG} and ρ_T from the equations (14), (24) and (40) respectively.

Using the conservation equations (5) and (6), we calculate the interaction as given below,

$$\begin{aligned}
Q = -\frac{3\rho_T}{1 + ka^{3n}} \sqrt{\frac{\rho_T}{3} \left(1 - \frac{\rho_T}{\rho_1} \right)} \left[\frac{1}{1 + ka^{3n}} \left(ka^{3n} (n + 1) + 1 - k^{-\alpha} \left(\frac{\rho_T}{1 + ka^{3n}} \right)^{-(\alpha+1)} a^{-3n\alpha} \right. \right. \\
\left. \left. \left(C' + \left(\left(\frac{ka^{3n} \rho_T}{1 + ka^{3n}} \right)^{1+\alpha} - C' \right)^{-\omega} \right) \right) - 1 \right] \quad (70)
\end{aligned}$$

From figs. 15 to 28 we have demonstrated the \dot{R} and mass curves for LQC. Here the \dot{R} for DM collapse is increasing in magnitude with time. But the mass is decreasing. The fact that the velocity of inward collapse is increasing but mass is decreasing, is quite an awkward incident to explain. This is a very unique property for LQC. In figs.17 and 18, we see the DE collapse in the universe filled up with MCG. The inward velocity with time whereas the mass of the collapsing centre decreases. The same result is followed for GCCG case in graphs figs.19 and 20. Unlike DGP case in LQC DM and DE combined case is dominated by the speedy collapse and decreasing mass incident.

5 Detailed Graphical Analysis

In the above figures the time derivative of the geometrical radius(\dot{R}) of the collapsing object and the mass(M) of the same have been plotted against time, for all the above cases. From the plots it is evident that the time derivative of the radius inevitably takes negative values, which in turn shows that the radius decreases with time, thus resulting in gravitational collapse. We discuss the graphs for the two sections separately in detail.

DGP BRANE MODEL

From the first figure we see that there is a considerable decrease in the value of \dot{R} , towards more negative values in the presence of dark matter(dust) only. This shows that matter field collapses due to their inward gravitational pull, and gradually increases in mass by accumulating more matter, which is evident from fig.2.

From fig.3, it is seen that in the presence of dark energy in the form of MCG, value of \dot{R} increases with time and has a gradual tendency of stepping into the positive region. This is due to the fact that the large negative pressure of the DE does not facilitate collapse under normal conditions. Initially if the space-time is trapped, during evolution it gets un-trapped and eventually the cloud shows a tendency to expand due to the presence of DE in the form of MCG. Even if the cloud does not expand, due to its local condensation, the time for formation of the apparent horizon and consequently a BH will be much delayed in future. Hence the formation of BH is quite an uncertainty, if at all it is a possibility. Fig.4 shows that due to DE accretion on the collapsing object, there is a gradual decrease in its mass, with time. With GCCG as the DE the story is almost the same, as is evident from figures 5 and 6. Fig. 7 shows that in the absence of any interaction, a combination of MCG and dust undergoes a sudden collapse, forming a singularity of the space-time. As expected there is a decrease in mass due to presence of DE in fig.8. In the presence of interaction neither DM nor DE(MCG) can dominate over each other, and hence we observe a mean behaviour between the two in fig.9. From fig.10 it is evident that there is an increase in mass with time. The reason being that interaction between DE and DM alleviates the DE accretion phenomenon on the collapsing object, thus preventing the mass from decreasing with time. With GCCG as DE we get almost identical scenario as MCG, in the absence of interaction with DM, which is evident from figs.11 and 12. In the presence of interaction, we get a slightly different situation in case of GCCG as far as mass is concerned. In fig.14 we see that there is a gradual decrease of mass, thus showing the dominance of DE over DM, unlike the case of MCG. This is characteristic of GCCG. The above results are obtained by considering large values for r_c , the cross over scale, since for small values of r_c , there is no theoretical possibility for a collapse.

LOOP QUANTUM COSMOLOGY MODEL

From fig.15 we see that there is at first a gradual decrease and then a steep decrease of mass due to collapse of DM in LQC model. This result is totally different from the corresponding result for DGP brane model. This is indeed quite surprising. The gravitational pull in case of LQC can be speculated to be really weak compared to other gravity theories. Fig.16 is quite obvious. Collapse with MCG in LQC is exhibited in figs. 17 and 18. The results obtained tally with the results obtained for DGP brane model. The only difference being that in case of LQC the graph for \dot{R} rises more steeply than in case of DGP brane. This again reflects on the weakness of gravity, speculated in the previous figs. Figs.19 and 20 characterizes the collapse of GCCG in LQC. Here also the results are similar to that of DGP brane model, the only difference being the steepness of the slope in LQC just like the previous graphs. Figs.21 and 22 shows the plots for combination of MCG and DM in the absence of interaction. Unlike DGP brane model in fig.21 there is no sudden collapse. In fact the increase in value of \dot{R} shows the dominating nature of DE over DM. The large negative pressure of MCG prevails over the weak gravity of DM, and hence there is a comparatively lesser tendency of collapse. Fig.22 shows decrease of mass with time, due to MCG accretion on the collapsing cloud. In presence of interaction MCG and DM show much moderate behaviour as is evident from the figs.23 and 24. Association with each other suppress their individual behaviour upto a great extent, thus bringing their mean properties to light. From figs.25 and 26 we get the characteristics of collapse with DM and GCCG as DE. Here also unlike DGP brane model there is no possibility of a sudden collapse, thus showing the dominance of DE over DM. Finally in figs.27 and 28 we consider collapse with GCCG and DM in presence of interaction. Unlike the case of MCG, in this case there is a greater possibility of collapse as seen from the figs.

Hence in case of LQC, the effect of MCG is felt upto a much greater extent than the effect of GCCG when combined with DM. This is characteristic of the two fluids and solely depend on their respective pressures. The above results are obtained on considering large values for ρ_1 , the critical loop quantum density, since for small values of ρ_1 there is no theoretical possibility of collapse.

6 Discussions and Concluding Remarks

Here we have studied the gravitational collapse of a spherically symmetric dust cloud of finite radius, filled with homogeneous and isotropic fluid. The study was carried out separately in two different types of modified gravity theories, namely DGP brane model and Loop quantum cosmology model in the background of a unified model of DE and DM. Two candidates for DE has been considered separately, namely modified Chaplygin gas and Generalized Cosmic Chaplygin gas. At first the effect of DM and DE(both MCG and GCCG) was studied separately and then their combined effect was studied both in the presence and absence of interaction. Values

for relevant parameters (time derivative of radius and mass of the collapsing cloud) were found out and their variations with time was plotted. A detailed graphical analysis was done to get a comparison between the results obtained in the two different models.

It was seen that in case of DM, there is a high possibility for the matter cloud to undergo collapse, and the consequent formation of a BH was inevitable, for both DGP and LQC models. In the background of DE, i.e., MCG or GCCG, the cloud shows a reluctance to undergo collapse, due to the high negative pressure of the DE fluids. If at all there is any possibility of a collapse and subsequent formation of a BH, it will be much delayed in future. Hence the formation of BH is absolutely an uncertain phenomenon in this case. This phenomenon is much more pronounced in LQC model than in the DGP brane model, thus showing the relative weakness of gravity in the LQC model compared to the DGP brane model. This is a very interesting result indeed. In the unified model of DE and MCG in the absence of interaction, there is a sudden collapse showing the dominance of matter over DE in the DGP model. Hence the fate of the collapse is a BH. But we have a completely different scenario for LQC model, where there is no such collapse showing the dominance of DE and the weakness of gravity. In the presence of interaction we see a moderation as far as the individual effects of DM and DE are concerned. The presence of either of them suppress the extremeness of their behaviour, as individuals. In all the above cases the presence of DE decreases the mass of the cloud due to DE accretion on it. In case of DM only there is an increase in mass due to accumulation of more matter.

Acknowledgement:

The authors are thankful to IUCAA, Pune, India for warm hospitality where part of the work was carried out.

References

- [1] Perlmutter, S. et al. :- [**Supernova Cosmology Project Collaboration**], *ApJ* **517**, 565(1999) [*arXiv:astro-ph/9812133*].
- [2] Spergel, D. N. et al. :- **WMAP Collaboration**, *Astron. J. Suppl* **148**, 175(2003) [*arXiv:astro-ph/0302209*].
- [3] Riess, A. G. et al. :- [**Supernova Search Team Collaboration**], *ApJ* **607**, 665(2004) [*arXiv:0402512*(astro-ph)].
- [4] Kamenshchik, A., Moschella, U. and Pasquier, V. :- *Phys. Lett. B* **511**, 265(2001).
- [5] Gorini, V., Kamenshchik, A. and Moschella, U. Pasquier, V. :- [*arXiv:0403062*(gr-qc)].
- [6] Gorini, V., Kamenshchik, A. and Moschella, U. :- *Phys. Rev. D* **67**, 063509(2003).
- [7] Alam, U., Sahni, V., Saini, T. D., Starobinsky, A.A. :- *MNRAS* **344** 1057(2003).
- [8] Bento, M. C., Bertolami, O., Sen, A. A. :- *Phys. Rev. D* **66**, 043507(2002).
- [9] Benaoum, H. B.:- [*arXiv:0205140*(hep-th)].
- [10] Debnath, U., Banerjee, A., Chakraborty, S. :- *Class. Quantum. Grav.* **21**, 5609(2004).
- [11] Setare, M. R. :- *Phys.Lett B* **648**, 329 (2007).
- [12] Setare, M. R. :- *Eur. Phys. J. C* **52** 689(2007).
- [13] Setare, M. R. :- *IJMPD* **18** 419(2009).
- [14] Barreiro, T.et. al.:- *Phys. Rev. D* **78** 043530(2008).
- [15] Makler, M. et. al.:- *Phys. Lett. B* **555** 1(2003).
- [16] Lu, J. et. al., *Phys. Lett. B* **662** (2008) 87.
- [17] Dao-Jun, L., Xin-Zhou, L. :- *Chin. Phys. Lett.* **22** 1600(2005).

- [18] Jing, H. et. al.:- *Chin. Phys. Lett.* **25** 347(2008).
- [19] Debnath, U. :- *Astrophys. Space Sci.* **312**, 295 (2007).
- [20] Panotopoulos, G. :- *Phys. Rev. D* **77** 107303(2008).
- [21] Gonzalez-Diaz, P.F.:- *Phys. Rev. D* **68**021303(R)(2003).
- [22] Chakraborty, W., Debnath, U., Chakraborty,S. :- *Grav. Cosmol.* **13**294(2007) [*arXiv:0711.0079[gr-qc]*].
- [23] Oppenheimer, J. R., Snyder, H. :- *Phys. Rev. D* **56** 455(1939).
- [24] Dvali, G. R. , Gabadadze, G., Porrati, M.:- *Phys.Lett. B* **485** 208(2000)[*arXiv:000506(hep-th)*].
- [25] Deffayet, D.:- *Phys.Lett. B* **502** 199(2001).
- [26] Deffayet, D., Dvali, G.R., Gabadadze, G.:-*Phys.Rev.D* **65** 044023 (2002)[*arXiv:0105068(astro-ph)*].
- [27] Cai, R.G., Wang, A. :- *J. Cosmol. Astropart. Phys.* **0503**002(2005)
- [28] Cai, R.G., Wang, A. :- *Phys.Rev. D* **73** 063005(2006).
- [29] Rovelli, C. :- *liv. Rev. Rel.* **11**(1998)
- [30] Ashtekar, A., Lewandowski, J. :- *Class. Quantum. Grav.* **21**R53(2004)
- [31] Ashtekar, A. :- *AIP Conf. Proc.* **8613**(2006)
- [32] Bojowald, M. :- *liv. Rev. Rel.* **8**11(2005)
- [33] Ashtekar, A. et al :- *Adv. Theor. Math. Phys.* **7**233(2003)
- [34] Wu, P., Jhang, S.N., :- *JCAP* **06**007(2008)
- [35] Wu, P., Yu, H. :- *Class. Quantum. Grav.* **24**, 4661(2007).
- [36] Chen, S., Wang, B., Jing, J. :- *Phys. Rev. D* **78** 123503(2008).
- [37] Fu, X., Yu, H., Wu, P. :- *Phys. Rev. D* **78** 063001(2008).